EDGE ARTICLE

Check for updates

Unlocking ultra-low temperature performance: an anti-freezing, high-conductivity, biodegradable hydrogel electrolyte for supercapacitors down to −60 °C

Yibin Xing, Nannan Zhu, Ruixi He, Xiyao Wang, Renyang Han, Bing Du and Xuejuan Wan [ID] *

Hydrogel electrolytes are highly regarded in supercapacitors for their intrinsic safety and mechanical adaptability, but inevitable freezing at subzero temperatures leads to rapid deterioration of electrochemical performance. To overcome this critical limitation, a freeze-resistant hydrogel electrolyte (SCG-Zn) capable of operating at ultra-low temperatures is developed by integrating biodegradable polysaccharides (sodium hyaluronate and carboxymethyl chitosan), glycerol, and zinc chloride. The synergistic effect of intense chloride ion (Cl^-) hydration and abundant hydrophilic groups (*e.g.*, −OH, −COOH, and −NH_2) within the hydrogel electrolyte creates a strongly bound water network, significantly suppressing ice crystallization and depressing the freezing point. This unique structure enables SCG-Zn to maintain exceptional ionic conductivity (13.32 mS cm^{-1}) even at −60 °C (35.75 mS cm^{-1} at 25 °C), arising from its high density of zincophilic functional groups and the establishment of continuous Zn^{2+} ion conduction pathways. Supercapacitors assembled with SCG-Zn electrolyte demonstrate exceptional cycling stability, retaining 97.6% capacity after 20 000 cycles at 25 °C. Impressively, even under the harsh condition of −60 °C, facilitated by the sustained ionic conduction of SCG-Zn, a remarkably high-capacity retention of 97.4% is achieved after 20 000 cycles. Furthermore, the assembled flexible devices also exhibit stable performance under repeated mechanical deformations (bending and loading). This work establishes a simple, sustainable but highly effective material for high-performance, reliable energy storage devices capable of operating in extreme cold environments.

Introduction

Flexible supercapacitors stand out among energy storage devices due to their high-power density, rapid charging/discharging capabilities, long cycle life, and excellent flexibility, finding widespread applications in portable electronic devices, medical equipment, and curved displays.[1–5] Hydrogels, owing to their superior flexibility and interface compatibility, have emerged as promising candidates for electrolytes in flexible supercapacitors.[6] However, hydrogel electrolytes contain a significant amount of free water, which inevitably freezes at sub-zero temperatures.[7,8] This significantly reduces ion mobility and the flexibility of the hydrogel and even leads to device failure. Conventional strategies to enhance the freeze resistance of hydrogel electrolytes primarily involved additive engineering and polymer network design. Additive engineering typically employs hydrophilic polyols (*e.g.*, glycerol and ethylene glycol),[9,10] polar organic solvents,[11] ionic liquids,[12] or high

concentrations of salt[13,14] as cryoprotectants to restrict the mobility of free water and depress the freezing point. Chen *et al.* developed an HC-SiO$_2$ electrolyte using a high-concentration dual-salt system (1 M Zn(OAc)$_2$ and 21 M LiCl), and the assembled devices demonstrate high capacity at −20 °C.[15] Nevertheless, ionic conductivity in such systems typically undergoes an order-of-magnitude reduction below −40 °C, revealing application limitations at ultra-low temperatures. Polymer network design mainly focuses on developing matrices with strong hydrogen bond donors (*e.g.*, −OH, −COOH, and −NH$_2$) to immobilize water molecules and inhibit ice crystal nucleation, while simultaneously incorporating zincophilic groups (−SO$_3$H) to optimize Zn^{2+} transport pathways.[16,17] Mo *et al.* developed an EG-modified waPUA/PAM hydrogel electrolyte, in which intensive polymer–water hydrogen bonding inhibits ice crystallization, enabling stable operation at low temperatures down to −20 °C.[18] However, concurrently achieving high mechanical strength, low frost resistance temperature and superior ionic conductivity also remains challenging solely through hydrogel network design, with operational temperatures rarely extending beyond −40 °C.

College of Materials Science and Engineering, Shenzhen University, Shenzhen 518060, China. E-mail: wanxj@szu.edu.cn

Additionally, it is worth noting that most reported hydrogel electrolytes rely on non-biodegradable synthetic polymers, posing persistent environmental risks. Developing biodegradable alternatives from biomass-derived polymers (*e.g.*, cellulose derivatives, chitosan, sodium alginate, and agarose) represents a promising strategy toward eco-friendly flexible electrochemical energy storage devices.[19,20] Zhu *et al.* engineered a low-temperature self-healing hydrogel electrolyte *via* peach gum and silk nanofiber, and the assembled supercapacitor maintains >90% capacity after 15 000 cycles at −20 °C.[21] However, its low-temperature ionic conductivity is limited to 1.36 mS cm^{-1}, which strongly hinders its cold-environment applications. So far, despite significant advances in biomass-derived hydrogel electrolytes,[22,23] a critical challenge remains in concurrently achieving ultrahigh freeze-resistant stability (operation below −40 °C) and competitive low-temperature ionic conductivity.

To address ultra-low temperature operational challenges, we developed an antifreeze biodegradable hydrogel electrolyte comprising sodium hyaluronate (SH), carboxymethyl chitosan (CMCS), glycerol and ZnCl$_2$ (denoted as SCG-Zn) for flexible supercapacitors. The synergistic interaction between carboxyl-rich biopolymers (SH/CMCS) and Zn^{2+} ions establishes a robust cross-linked network, enhancing the mechanical stability of the hydrogel electrolyte and simultaneously facilitating efficient zinc ion transport.[24,25] The integration of glycerol further improves the flexibility and interfacial adhesion of the hydrogel electrolyte, facilitating interfacial contact between the electrolyte and electrodes. The high ZnCl$_2$ loading endows it with outstanding freeze resistance. Remarkably, supercapacitors assembled with SCG-Zn exhibit exceptional cryogenic cycling stability, maintaining a high-capacity retention rate of 97.4% after 20 000 cycles at −60 °C. The supercapacitors also maintain stable electrochemical performance and high cycling stability during cyclic temperature variations from −60 °C to 40 °C, demonstrating excellent long-term cycling stability. The assembled flexible supercapacitor operates stably under
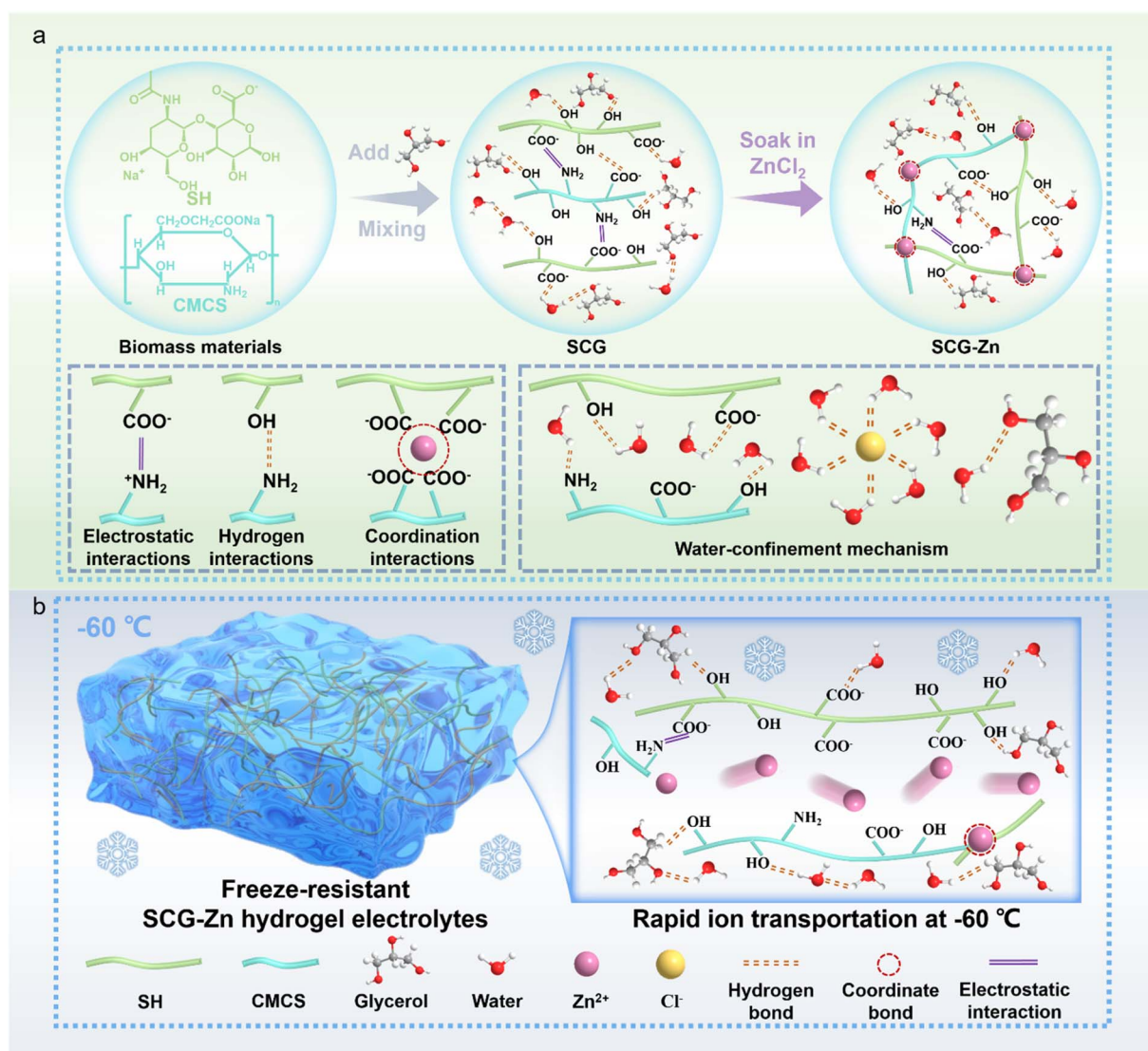

Fig. 1 Schematic illustrations of (a) the SCG-Zn hydrogel electrolyte, its intermolecular interactions, and water confinement mechanism. (b) The ion transport mechanism at −60 °C within the SCG-Zn hydrogel electrolyte.

repeated mechanical deformation, demonstrating its viability for energy storage in extreme environments.

Results and discussion

The SCG-Zn hydrogel electrolyte was fabricated using the natural polysaccharides SH and CMCS, which self-assembled into a dynamic network *via* electrostatic attraction and hydrogen bonding (Fig. 1a and S1). To enhance the hydrogel flexibility, glycerol was incorporated, which simultaneously increased the density of hydrophilic groups within the matrix. Subsequent immersion in concentrated $ZnCl_2$ solution induced coordination crosslinking where Zn^{2+} ions bridged carboxyl groups (–COOH) throughout the network. This dynamic dual-network architecture, integrating hydrogen bonding, electrostatic interactions and coordination crosslinking, endows the SCG-Zn hydrogel electrolyte with robust mechanical properties. Furthermore, the abundant hydrophilic functional groups, synergistically combined with the strong hydration capability of chloride ions, collectively facilitate the conversion of free water into bound water through hydrogen bonding and ion hydration effects, significantly enhancing the hydrogel's water retention and freeze-resistance capacity. As illustrated in Fig. 1b, the high density of zinc-affinity functional groups (*e.g.*, –COO⁻ and NH_2) within the SCG-Zn hydrogel establishes continuous ion-hopping channels that enable rapid Zn^{2+} migration. Remarkably, the synergistic effects of its superior freeze resistance allow efficient ion transport even at −60 °C, facilitating energy storage device operation under ultra-low temperature environments.

The compositional and structural characteristics of the SCG-Zn hydrogel electrolyte were further investigated. Fourier transform infrared (FTIR) spectroscopy (Fig. 2a) confirmed the critical functional groups of SH, including O–H stretching (3263 cm^{-1}) and asymmetric –COO⁻ stretching (1602 cm^{-1}), while CMCS displayed N–H stretching (3290 cm^{-1}) and asymmetric –COO⁻ stretching (1583 cm^{-1}). Crucially, coordination between Zn^{2+} ions and carboxylate groups was evidenced by a blue shift in the asymmetric –COO⁻ stretch from 1604 cm^{-1} (SCG) to 1621 cm^{-1} (SCG-Zn). X-ray photoelectron spectroscopy (XPS) analysis further substantiated this coordination, revealing a Zn 2p peak at 1023.56 eV (Fig. 2b) corresponding to Zn–O bonds. High-resolution spectra (Fig. 2c–e) confirmed key bonding environments: C 1s featured C–O/C–N (287.15 eV) and O=C–O (288.82 eV); O 1s resolved into O=C (532.38 eV) and O–C (533.93 eV); and N 1s comprised N–H (400.84 eV) and C–N (402.88 eV) species. X-ray diffraction (XRD) analysis (Fig. 2f)
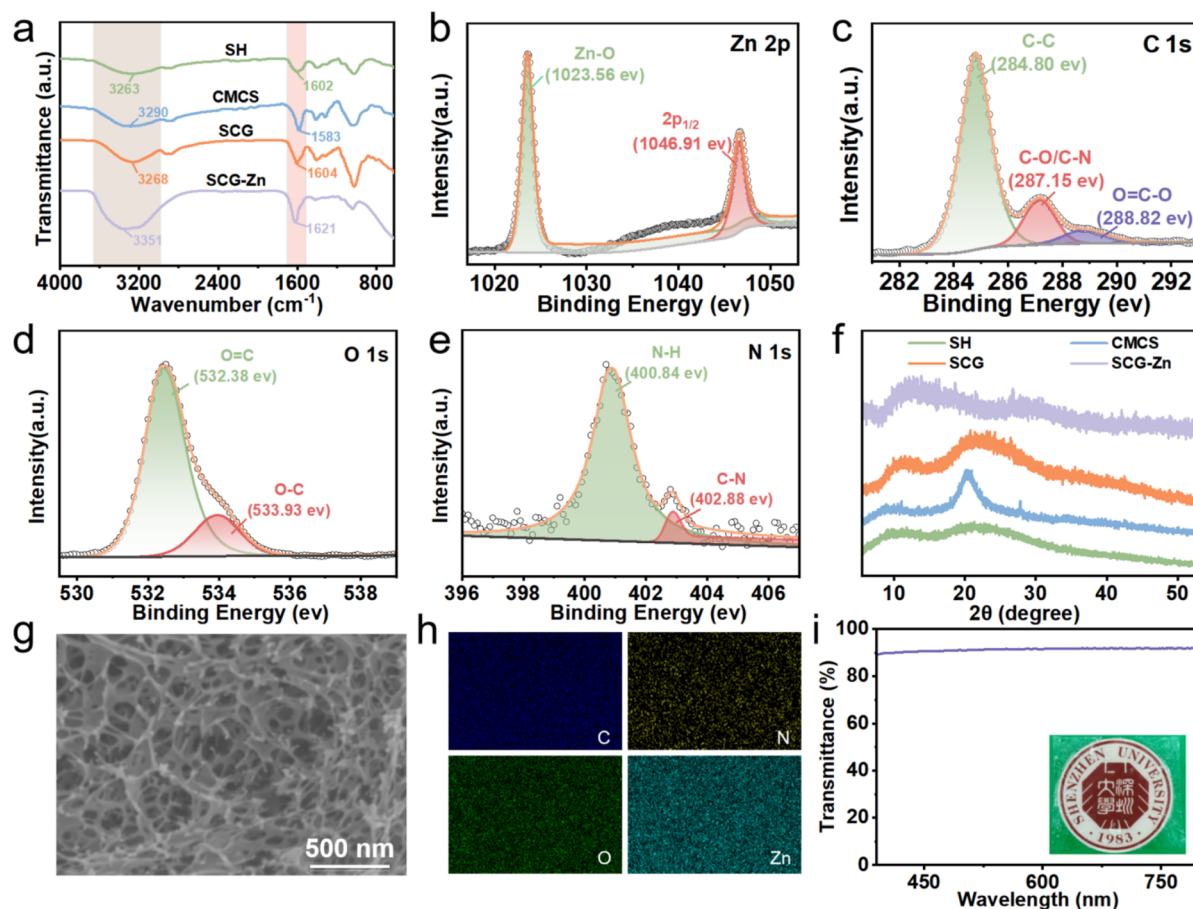

Fig. 2 (a) FTIR spectra of SH, CMCS, SCG and SCG-Zn. (b–e) XPS spectra of the Zn 2p, C 1s, O 1s and N 1s of the SCG-Zn hydrogel. (f) XRD spectra of SH, CMCS, SCG and SCG-Zn. (g) Cross-sectional SEM image and (h) elemental distribution of SCG-Zn. (i) UV-vis transmittance spectrum of SCG-Zn (inset showing its optical photograph).

revealed a broad amorphous halo at $\sim10°$ for SCG-Zn, confirming a disordered polymer matrix without crystalline phases. Scanning electron microscopy (SEM) images of the SCG-Zn cross-section revealed an interconnected porous architecture (Fig. 2g), directly facilitating rapid ion transport. Elemental mapping verified homogeneous spatial distribution of carbon (C), nitrogen (N), oxygen (O), and zinc (Zn) throughout the hydrogel network, confirming compositional uniformity (Fig. 2h). Moreover, SCG-Zn exhibited exceptional optical transparency (>89.9% transmittance across the visible spectrum; Fig. 2i), enabling real-time observation of the electrolyte–electrode interface during device assembly.

The operational stability of supercapacitors at low temperatures is critical for their widespread application, which is intrinsically governed by the water retention capacity and anti-freezing properties of hydrogel electrolytes. Fundamentally, water freezing constitutes a phase transition from a disordered liquid to an ordered crystalline state, mediated by hydrogen bond (HB) reorganization. Strategic disruption of water's hydrogen-bonding network *via* high-concentration salts can effectively depress the freezing point, as validated by differential scanning calorimetry (DSC) in Fig. 3a. The anti-freezing behavior of SCG membranes immersed in 2 M $ZnSO_4$ and $ZnCl_2$ (2–5 M) solutions revealed distinct responses. Compared to $ZnSO_4$-immersed counterparts, $ZnCl_2$ systems exhibit lower
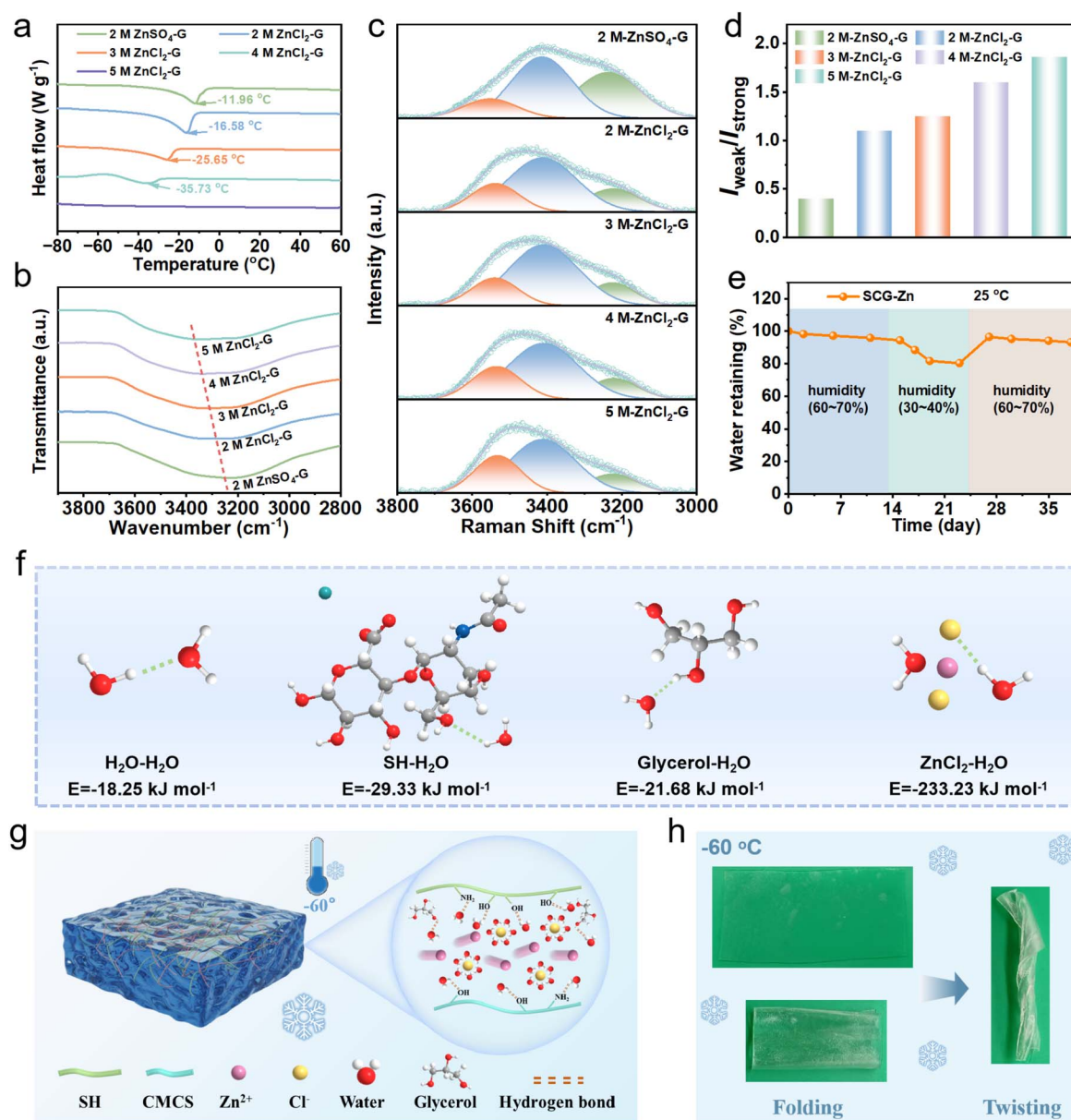

Fig. 3 SCG hydrogel electrolytes with $ZnSO_4$ or $ZnCl_2$: (a) freezing points, (b) FTIR spectra (2800–3900 cm^{-1}), (c) deconvoluted O−H stretching vibrations in Raman analysis showing H_2O hydrogen-bonding states (strong/medium/weak), and (d) weak-to-strong hydrogen-bond intensity ratio. (e) Water retention of SCG-Zn at 25 °C. (f) DFT-calculated H_2O binding energies with H_2O, SH, glycerol, and $ZnCl_2$. (g) Proposed anti-freezing mechanism. (h) Deformation tolerance (folding/twisting) at −60 °C.

freezing points, which progressively decrease with increasing concentration. Critically, at a 5 M ZnCl₂ concentration, the absence of an ice-melting peak indicated the complete suppression of ice formation, suggesting superior freeze resistance. The freeze-resistant mechanism of SCG-Zn hydrogel electrolyte was further characterized by various spectroscopic analyses. FTIR spectra revealed a continuous blue shift of O–H stretching vibration with increasing concentration of the electrolyte salt (Fig. 3b), indicating reduced hydrogen-bonded water clusters due to ionic solvation shell formation.[26] Gaussian curve fitting of the 2800–3900 cm^{-1} region resolved the spectrum into three components (Fig. S2a). The calculated peak areas (Fig. S2b) showed an increase in the weak HB-associated area with increasing ZnCl₂ concentration, consistently exceeding that of the 2 M ZnSO₄ sample. To further elucidate HB evolution, the broad O–H stretching vibration peak (3000–3800 cm^{-1}) in Raman spectroscopy was also deconvoluted into three distinct components: strong O–H stretching (∼3230 cm^{-1}), medium O–H stretching (∼3430 cm^{-1}), and weak O–H stretching (∼3600 cm^{-1}) (Fig. 3c). Gaussian fitting quantified an increasing trend in the weak-to-strong HB ratio (I_{weak}/I_{strong}) with higher ZnCl₂ concentration (Fig. 3d), surpassing that of the 2 M ZnSO₄ system. This trend reflects hierarchical HB reconstruction, wherein chloride ions preferentially disrupt tetrahedral/cyclic HB structures that template ice nucleation (dominating at ∼3230 cm^{-1}), leading to disordered, weaker hydrogen bonds instead.[27] Owing to the strong interactions between system components and water molecules, the SCG-Zn hydrogel electrolyte exhibits exceptional water retention capabilities. Thermogravimetric analysis (TGA) in Fig. S2c reveals a water content of 36.69% in SCG-Zn. At room temperature and 60–70% humidity, it retains 94.32% mass after 15 days of storage (Fig. 3e). Subsequent storage at 30–40% humidity led to the reduction of mass retention to 80.27% after one week; however, re-exposure to higher humidity (60–70%) enabled its rapid recovery to 96.45% of initial mass, demonstrating the hydrogel's superior rehydration capacity. A further week of storage maintained 93.15% water retention, attributed to abundant hydrophilic functional groups within the electrolyte. Binding energy ($E_{binding}$) calculations provide a quantitative measure of intermolecular interaction strength, where more negative values indicate greater stabilization. In the SCG-Zn hydrogel electrolyte, numerous water-binding components with high negative $E_{binding}$ effectively suppress HB formation and depress the freezing point by hindering water reorganization into crystalline structures. As shown in Fig. 3f, the $E_{binding}$ values for SH-H₂O (−29.33 kJ mol^{-1}), glycerol-H₂O (−21.68 kJ mol^{-1}), and ZnCl₂–H₂O (−233.23 kJ mol^{-1}) were all lower than that for H₂O–H₂O (−18.25 kJ mol^{-1}), confirming that water molecules preferentially interact with SH, glycerol, and ZnCl₂ rather than self-associating. Notably, the significantly lower $E_{binding}$ of ZnCl₂–H₂O highlights its superior efficacy in disrupting water–water HBs. These results collectively demonstrate the exceptional anti-freezing performance of the SCG-Zn hydrogel electrolyte: a synergistic effect between its hydrophilic functional groups (–OH, –COO$^-$, etc.) and the strong electronegativity of chloride ions, which disrupts the inherent

water HB network, thereby lowering the freezing point (Fig. 3g). Direct observation of hydrogels immersed in different salt solutions visually confirmed their anti-freezing capability (Fig. 3h and S3). Even at −60 °C, the hydrogel electrolyte with 5 M ZnCl₂ retained flexibility and could withstand severe deformation (folding/bending) (Fig. 3h), ascribed to the strong hydration by Cl$^-$ ions that generates substantial unfrozen bound water. In contrast, the ZnSO4-immersed hydrogel froze at −60 °C.

Interestingly, without glycerol addition, the SC hydrogel showed similar anti-freezing trends: its freezing point also progressively decreased with increasing ZnCl₂ concentration, consistently outperforming the 2 M ZnSO₄ system (Fig. S4a). Consistent with the SCG system, the FTIR spectra of the SC hydrogel exhibited continuous blue-shifting O–H vibrations (Fig. S4b), while Gaussian fitting confirmed steadily increasing proportions of weak hydrogen bonds at higher ZnCl₂ concentration. Notably, this proportion remains lower than that in the glycerol-containing SCG hydrogel (Fig. S4c–f). However, excessive ZnCl₂ concentrations can induce ion-pair aggregation in the polymer matrix, leading to significant conductivity degradation (Fig. S5a–c) and reduced elasticity (Fig. S5d and e). To balance low-temperature toughness with electrochemical and mechanical performance, glycerol was introduced as a multifunctional plasticizer. Its incorporation synergistically enhanced chain mobility and facilitated ion transport, achieving a peak conductivity of 35.75 mS cm^{-1} at 30 wt% glycerol (Fig. S6a–c). Mechanical characterization confirmed that this formulation optimizes the synergy between flexibility and strength, achieving exceptional elongation (207.4 kPa) without sacrificing tensile strength (the modulus is 858.7 Pa) (Fig. S6d). These results indicated that the high-concentration salt played the dominant role in imparting freeze resistance, while glycerol served a beneficial role by improving the flexibility of the hydrogel electrolyte.

The inherent self-adhesive property of the hydrogel electrolyte enables intimate interfacial coupling with electrodes, an essential requirement for minimizing interfacial impedance under mechanical deformation and maintaining electrochemical stability. As shown in Fig. 4a, the SCG-Zn hydrogel electrolyte exhibited effective adhesion to diverse substrates, including metal foils (zinc, copper, steel, and titanium), paper, and a leaf. Notably, a hydrogel layer sandwiched between two paper sheets (adhesion area: 3 × 1 cm^2) could sustain a 200 g weight. Quantitative tensile tests (Fig. 4b) revealed that the adhesion strengths of the SCG-Zn hydrogel were 18.5 kPa (zinc foil), 14.7 kPa (copper foil), 23.4 kPa (steel foil), 24.4 kPa (titanium foil), and 36.8 kPa (paper), respectively (Fig. 4c), surpassing previously reported biomass-derived hydrogel electrolytes (Fig. 4d).[7,28–31] This exceptional adhesion originates from multiple dynamic interfacial interactions, such as hydrogen bonding and metal–ligand coordination (Fig. 4e). The SCG-Zn hydrogel maintains adhesion capacity even at −60 °C, ensuring reliable interfacial contact for stable supercapacitor operation under extreme conditions (Fig. S7). Optical microscopy confirmed that the SCG-Zn hydrogel electrolyte maintained firm adhesion to the electrodes without delamination,
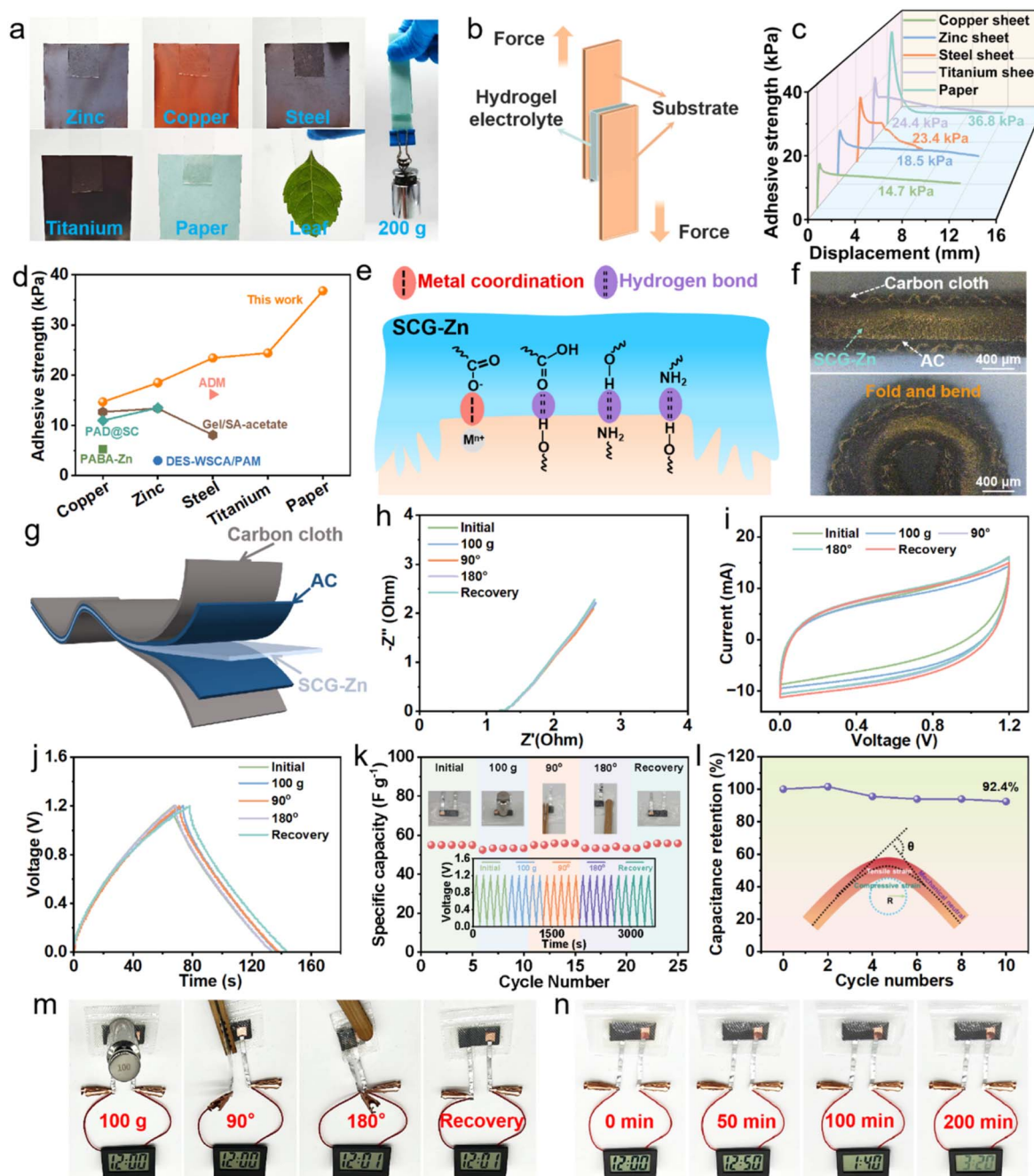
Fig. 4 Adhesion demonstration of SCG-Zn: (a) bonding to diverse substrates and the weight-bearing capacity (200 g) between two paper substrates, (b) diagram of the adhesion testing device, (c) adhesive strength on different substrates, (d) comparative adhesive strength *versus* reported hydrogels, and (e) proposed adhesion mechanism. (f) Optical observations for the electrode–hydrogel interface. (g) Schematic for the flexible supercapacitor. Electrochemical performance under deformation: (h) EIS plots, (i) CV curves (40 mV s^{-1}), (j) GCD profiles (0.5 A g^{-1}), and (k) cycling stability under different deformation/recovery cycles. (l) Capacitance retention under continuous bending. Powering an electronic watch by the flexible supercapacitor: (m) under various mechanical stimuli and (n) 200 min continuous power delivery.

even during bending (Fig. 4f). To further evaluate practical reliability, a flexible supercapacitor was assembled by sandwiching the SCG-Zn electrolyte between two carbon cloth electrodes (AC@CC), as depicted in Fig. 4g. The electrochemical performance of the flexible supercapacitor remained stable under various mechanical stimuli (100 g weight loading and 90°/180° bending) and subsequent recovery. Nearly overlapping

electrochemical impedance spectroscopy (EIS) curves indicated minimal internal resistance changes during loading or bending (Fig. 4h). Both cyclic voltammetry (CV) and galvanostatic charge–discharge (GCD) curves of the flexible supercapacitor (Fig. 4i–j) exhibited negligible shape distortion, reflecting excellent mechanical stability. The deformation/recovery cycles of the flexible supercapacitor in Fig. 4k showed no significant

capacitance loss, suggesting that the hydrogel electrolyte possesses favorable mechanical robustness, adhesion, and ion transport kinetics, which led to the superior electrochemical stability and mechanical adaptability of the device. The flexible supercapacitor retained 92.4% of its initial capacitance after 10 bending cycles (Fig. 4l) and could reliably power an electronic watch under various mechanical stimuli (Fig. 4m). A fully charged flexible supercapacitor could power an electronic timer for over 200 minutes (Fig. 4n).

Quasi-solid-state supercapacitors were fabricated by sandwiching the SCG-Zn hydrogel electrolyte between two activated carbon (AC) electrodes, and their electrochemical performance was evaluated. CV curves measured in various voltage windows and at different scan rates are shown in Fig. S8 and 5a, respectively. At a scan rate of 40 mV s^{-1}, the CV curves exhibited quasi-rectangular shapes within voltage windows ranging from 0–0.8 V to 0–1.4 V, indicating ideal electric double-layer capacitive behavior and rapid charge/discharge kinetics. A noticeable tailing extension was observed beyond 1.2 V, necessitating a 0–1.2 V window for subsequent electrochemical characterization. Furthermore, the CV profiles retained their quasi-rectangular shape even at high scan rates ranging from 20 mV s^{-1} to 300 mV s^{-1}, demonstrating exceptional rate stability. The electrochemical performance of the supercapacitor was systematically assessed across an extended temperature range (−60 °C to 80 °C) to evaluate its cryogenic resilience. EIS results of the SCG-Zn hydrogel electrolyte (Fig. 5b and S9) revealed gradually increasing resistance with decreasing temperature. The insets in Fig. 5b and S10 directly illustrate the correlation between the ionic conductivity of SCG-Zn and temperature. The ionic conductivity increased from 13.32 mS cm^{-1} at −60 °C to 40.38 mS cm^{-1} at 40 °C, surpassing most reported hydrogel
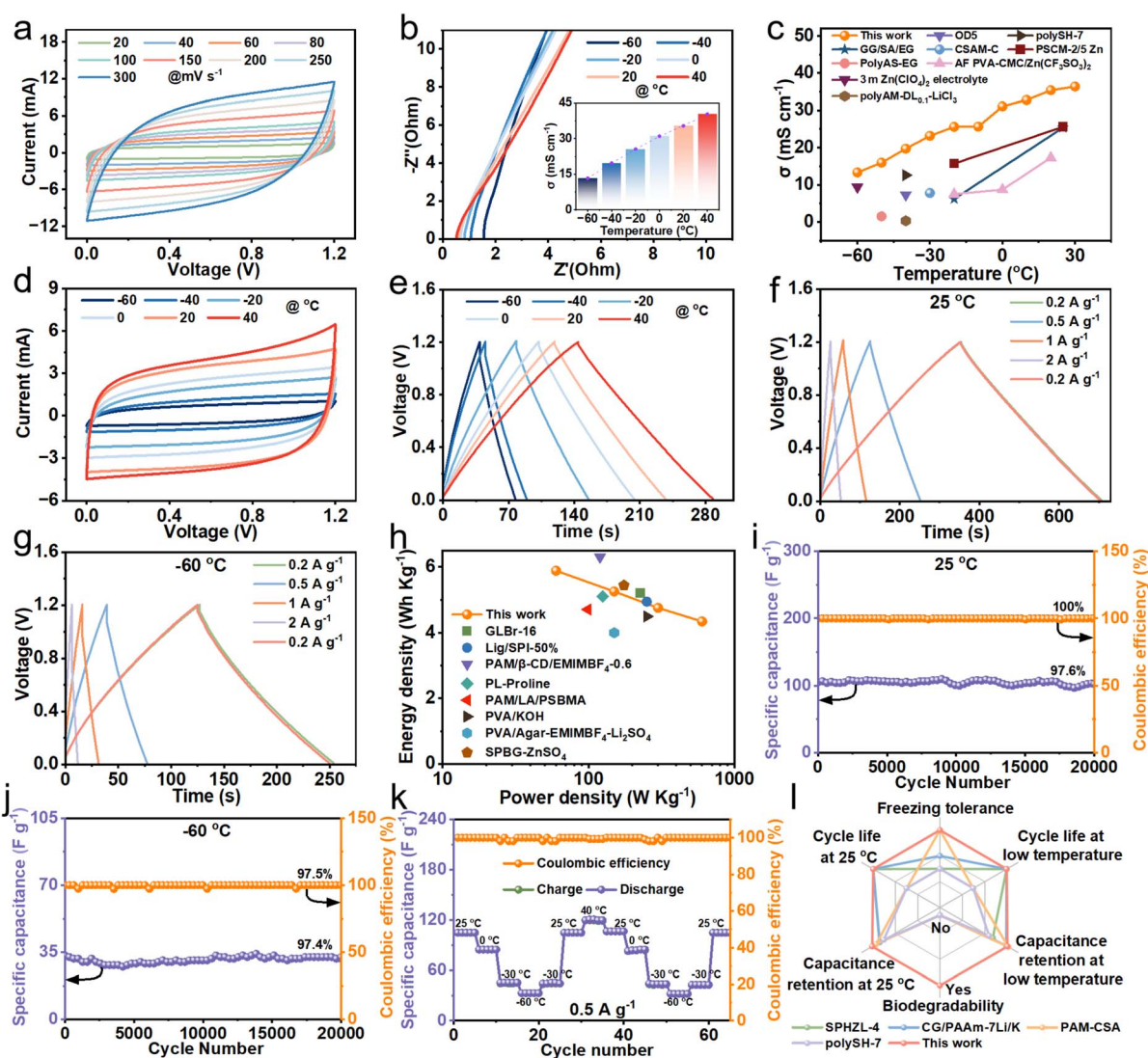

Fig. 5 Electrochemical performance of SCG-Zn based coin supercapacitors: (a) CV curves at varied scan rates, (b) EIS plots at different temperatures, (c) ionic conductivity in comparison with reported hydrogels, (d) CV curves (40 mV s^{-1}) and (e) GCD curves (0.5 A g^{-1}) at different temperatures. GCD curves at various current densities: (f) 25 °C and (g) −60 °C. (h) Ragone plot comparison. Cycling performance at 0.5 A g^{-1}: (i) 25 °C and (j) −60 °C. (k) Specific capacitance after thermal cycling (40 to −60 °C) following 20 000 cycles at −60 °C. (l) Performance comparison: freezing tolerance, cycling performance, and biodegradability.

electrolytes (Fig. 5c), especially under cryogenic conditions.[14,16,17,23,32–36] Furthermore, EIS measurements conducted after 14 days of exposure to ambient conditions revealed a marginal increase in internal resistance of only 0.23 Ω (Fig. S11a), while the ionic conductivity retained 65.88% of its initial value (Fig. S11b). Fig. 5d presents the CV curves of the supercapacitor at various temperatures. The reduced curve area under cryogenic conditions maintained a quasi-rectangular shape, demonstrating exceptional electrochemical stability at extreme temperatures. Correspondingly, GCD curves measured at 0.5 A g^{-1} across temperature gradients exhibited symmetrical triangular profiles (Fig. 5e), confirming highly reversible charge/discharge behavior at low temperatures.

Additionally, GCD measurements were performed across varying current densities at 25 °C, −30 °C, and −60 °C. As shown in Fig. 5f–g and S12, the GCD curves exhibited near-identical overlap with stable recovery of specific capacitance to the initial value (Fig. S13) after cycling the current density from 0.2 A g^{-1} to 2 A g^{-1} and returning to 0.2 A g^{-1}, demonstrating exceptional cryogenic resilience and rate performance. The supercapacitor delivered an energy density of 5.25 Wh kg^{-1} at a power density of 150 W kg^{-1} (25 °C, 0.5 A g^{-1}), surpassing most reported hydrogel-electrolyte-based supercapacitors (Fig. 5h).[10,21,37–42] Remarkably, it maintained high energy densities under extreme temperatures: 2.67 Wh kg^{-1} at −30 °C and 1.63 Wh kg^{-1} at −60 °C (both at 150 W kg^{-1}) (Fig. S14). Moreover, the supercapacitor exhibited outstanding cycling stability under extremely cold conditions, retaining 97.6% capacitance with near 100% coulombic efficiency after 20 000 cycles at 25 °C, 98.15% after 20 000 cycles at −30 °C, and critically, 97.4% after 20 000 cycles at −60 °C (Fig. 5i–j, and S15). Effective interfacial contact between the hydrogel electrolyte and electrodes minimized interfacial resistance growth, resulting in low voltage drops of 0.02 V at 25 °C, 0.09–0.13 V at −30 °C and 0.12–0.14 V at −60 °C after prolonged cycling (Fig. S16). To further assess cryogenic tolerance and cycling stability, the device first underwent 20 000 cycles at −60 °C, followed by thermal cycling between −60 °C and 40 °C (Fig. 5k). The specific capacitance exhibited stable recovery during repeated thermal cycling, highlighting superior cryogenic endurance and operational durability. Overall, the supercapacitor assembled with SCG-Zn achieves a significant breakthrough in critical performance metrics: cryogenic tolerance down to −60 °C, extended cycle life, and high capacitance retention. Meanwhile, SCG-Zn exhibited biodegradability and underwent nearly complete degradation (>95% mass loss) after 55 days of soil burial (Fig. S17). Further evidence of degradation occurring within the soil was demonstrated through tensile testing (Fig. S18). This exceptional performance significantly surpasses that of most reported hydrogel-based flexible supercapacitors (Fig. 5l),[14,43–45] positioning the device as a highly promising candidate for practical applications in extreme environments.

Conclusions

In summary, a biomass-derived hydrogel electrolyte (SCG-Zn) with exceptional cryogenic tolerance was successfully prepared via a straightforward method. Synergistic ionic coordination coupled with a dense hydrogen-bonding network endowed SCG-Zn with robust mechanical properties (a tensile strength of 200 kPa), favorable interfacial adhesion (36.8 kPa), superior water retention (≥35 days with 93.15% retention), and rapid zinc-ion transport capability (an ionic conductivity of 35.75 mS cm^{-1} at 25 °C). Particularly noteworthy was its outstanding freeze resistance, maintaining flexibility and high ionic conductivity (13.32 mS cm^{-1}) even at −60 °C. The assembled supercapacitor demonstrated a high-power density (150 W kg^{-1}) and energy density (5.25 Wh kg^{-1}) at 0.5 A g^{-1}, along with excellent cycling stability (retaining 97.6% capacitance after 20 000 cycles). Remarkably, an exceptional capacitance retention of 97.4% was maintained after 20 000 cycles at an extremely low temperature of −60 °C. Furthermore, this flexible supercapacitor maintained stable electrochemical performance under various mechanical stimuli (e.g., bending and weight-bearing). Overall, the developed freeze-resistant, biomass-derived hydrogel electrolyte presented a promising strategy for flexible energy storage devices operating in extreme environments.

Author contributions

Yibin Xing designed the experimental protocol, analyzed all data, and wrote the manuscript. Nannan Zhu assisted in testing and modifying the manuscript. Ruixi He, Xiyao Wang, and Renyang Han contributed to the interpretation of experimental results. Bing Du assisted in conceptualization and methodology. Xuejuan Wan conceptualised the research, established the methodology, reviewed and revised the manuscript, and secured funding. All authors commented on the manuscript and approved its submission.

Conflicts of interest

The authors declare no competing financial interests.

Data availability

The data supporting this article have been included as part of the SI.

Supplementary information: Preparation and characterization of SCG-Zn hydrogel electrolyte, details of performance testing and additional data. See DOI: https://doi.org/10.1039/d5sc05466d.

Acknowledgements

Notes and references

1 M. Pantrangi, E. Ashalley, M. K. Hadi, H. Xiao, Y. Zhang, W. Ahmed, N. Singh, A. Alam, U. Younis, F. Ran, P. Liang and Z. Wang, Flexible micro-supercapacitors: materials and architectures for smart integrated wearable and implantable devices, *Energy Storage Mater.*, 2024, **73**, 103791.

2 H. Dai, G. Zhang, D. Rawach, C. Fu, C. Wang, X. Liu, M. Dubois, C. Lai and S. Sun, Polymer gel electrolytes for flexible supercapacitors: recent progress, challenges, and perspectives, *Energy Storage Mater.*, 2021, **34**, 320–355.

3 J.-H. Lee, G. Yang, C.-H. Kim, R. L. Mahajan, S.-Y. Lee and S.-J. Park, Flexible solid-state hybrid supercapacitors for the internet of everything (IoE), *Energy Environ. Sci.*, 2022, **15**, 2233–2258.

4 S. V. Bhosale and S. V. Bhosale, Advancements in supercapacitors: breaking barriers and enabling amazing applications, *Chem. Sci.*, 2025, **16**, 10159–10227.

5 J. He, L. Cao, J. Cui, G. Fu, R. Jiang, X. Xu and C. Guan, Flexible Energy Storage Devices to Power the Future, *Adv. Mater.*, 2023, **36**, 2306090.

6 B.-H. Xiao, K. Xiao, J.-X. Li, C.-F. Xiao, S. Cao and Z.-Q. Liu, Flexible electrochemical energy storage devices and related applications: recent progress and challenges, *Chem. Sci.*, 2024, **15**, 11229–11266.

7 R. Hu, X. Yang, W. Cui, L. Leng, X. Zhao, G. Ji, J. Zhao, Q. Zhu and J. Zheng, An Ultrahighly Stretchable and Recyclable Starch-Based Gel with Multiple Functions, *Adv. Mater.*, 2023, **35**, 2303632.

8 Y. Shi, R. Wang, S. Bi, M. Yang, L. Liu and Z. Niu, An Anti-Freezing Hydrogel Electrolyte for Flexible Zinc-Ion Batteries Operating at -70 °C, *Adv. Funct. Mater.*, 2023, **33**, 2214546.

9 J. Liu, Q. Dang, J. Yuwono, S. Zhang, Z. Tai, Z. Guo and Y. Liu, Regulating the Coordination Environment of H_2O in Hydrogel Electrolyte for a High-Environment-Adaptable and High-Stability Flexible Zn Devices, *Nano-Micro Lett.*, 2025, **17**, 292.

10 S. Cui, W. Miao, X. Wang, K. Sun, H. Peng and G. Ma, Multifunctional Zincophilic Hydrogel Electrolyte with Abundant Hydrogen Bonds for Zinc-Ion Capacitors and Supercapacitors, *ACS Nano*, 2024, **18**, 12355–12366.

11 Y. Shi, Y. Guan, M. Liu, X. Kang, Y. Tian, W. Deng, P. Yu, C. Ning, L. Zhou, R. Fu and G. Tan, Tough, Antifreezing, and Piezoelectric Organohydrogel as a Flexible Wearable Sensor for Human–Machine Interaction, *ACS Nano*, 2024, **18**, 3720–3732.

12 Y. Chen, M. Zhu, C. Li, H. Wang, D. Chen, H. Wu, Z. Huang, Y. Wang, Y. Fan, Z. Bai, S. Chen, Y. Tang and Y. Zhang, Ionic Liquid-Based Hydrogel Electrolytes Enabling High-Voltage-Plateau Zinc-Ion Batteries, *Adv. Funct. Mater.*, 2025, 2501162, DOI: 10.1002/adfm.202501162.

13 C. Yan, Y. Wang, X. Deng and Y. Xu, Cooperative Chloride Hydrogel Electrolytes Enabling Ultralow-Temperature Aqueous Zinc Ion Batteries by the Hofmeister Effect, *Nano-Micro Lett.*, 2022, **14**, 98.

14 J. Yang, Z. Xu, J. Wang, L. Gai, X. Ji, H. Jiang and L. Liu, Antifreezing Zwitterionic Hydrogel Electrolyte with High Conductivity of 12.6 mS cm^{-1} at -40 °C through Hydrated Lithium Ion Hopping Migration, *Adv. Funct. Mater.*, 2021, **31**, 2009438.

15 M. Chen, G. Chen, C. Sun, X. Li, M. Zhang, H. Hua, J. Zhao and Y. Yang, SiO_2 Nanoparticles-Induced Antifreezing Hydrogel Electrolyte Enables Zn-I_2 Batteries with Complete and Reversible Four-Electron-Transfer Mechanisms at Low Temperatures, *Angew. Chem., Int. Ed.*, 2025, **64**, e202502005.

16 R. Li, W. Jia, J. Wen, G. Hu, T. Tang, X. Li, L. Jiang, M. Li, H. Huang and G. Fang, MXene/Zwitterionic Hydrogel Oriented Anti-freezing and High-Performance Zinc–Ion Hybrid Supercapacitor, *Adv. Funct. Mater.*, 2024, **34**, 2409207.

17 W. Sun, Z. Xu, C. Qiao, B. Lv, L. Gai, X. Ji, H. Jiang and L. Liu, Antifreezing Proton Zwitterionic Hydrogel Electrolyte *via* Ionic Hopping and Grotthuss Transport Mechanism toward Solid Supercapacitor Working at -50 °C, *Adv. Sci.*, 2022, **9**, 2201679.

18 F. Mo, G. Liang, Q. Meng, Z. Liu, H. Li, J. Fan and C. Zhi, A flexible rechargeable aqueous zinc manganese-dioxide battery working at −20 °C, *Energy Environ. Sci.*, 2019, **12**, 706–715.

19 J. Ding, Y. Yang, J. Poisson, Y. He, H. Zhang, Y. Zhang, Y. Bao, S. Chen, Y. M. Chen and K. Zhang, Recent Advances in Biopolymer-Based Hydrogel Electrolytes for Flexible Supercapacitors, *ACS Energy Lett.*, 2024, **9**, 1803–1825.

20 T. Xu, K. Liu, N. Sheng, M. Zhang, W. Liu, H. Liu, L. Dai, X. Zhang, C. Si, H. Du and K. Zhang, Biopolymer-based hydrogel electrolytes for advanced energy storage/conversion devices: Properties, applications, and perspectives, *Energy Storage Mater.*, 2022, **48**, 244–262.

21 N. Zhu, Q. Teng, Y. Xing, X. Wang, Z. Zhang and X. Wan, Biomass Hydrogel Electrolytes toward Green and Durable Supercapacitors: Enhancing Flame Retardancy, Low-Temperature Self-Healing, Self-Adhesion, and Long-Term Cycling Stability, *Nano Lett.*, 2024, **24**, 12442–12451.

22 X. Jia, X. Ma, L. Zhao, M. Xin, Y. Hao, P. Sun, C. Wang, D. Chao, F. Liu, C. Wang, G. Lu and G. Wallace, A biocompatible and fully erodible conducting polymer enables implanted rechargeable Zn batteries, *Chem. Sci.*, 2023, **14**, 2123–2130.

23 J. Wang, Y. Huang, B. Liu, Z. Li, J. Zhang, G. Yang, P. Hiralal, S. Jin and H. Zhou, Flexible and anti-freezing zinc-ion batteries using a guar-gum/sodium-alginate/ethylene-glycol hydrogel electrolyte, *Energy Storage Mater.*, 2021, **41**, 599–605.

24 J. Long, T. Han, X. Lin, Y. Zhu, J. Liu and J. Niu, A quasi-solid-state self-healing flexible zinc-ion battery using a dual-crosslinked hybrid hydrogel as the electrolyte and Prussian blue analogue as the cathode material, *Chem. Sci.*, 2024, **15**, 10200–10206.

25 K. Chen, Y. Xu, H. Li, Y. Li, L. Zhang, Y. Guo, Q. Xu, Y. Li and H. Xie, Design of cellulosic poly(ionic liquid)s with a hydrogen bond/ion dual regulation mechanism for highly reversible Zn anodes, *Chem. Sci.*, 2025, **16**, 8648–8660.

26 C. Tang, M. Li, Y. Yao, Y. Wang, Y. Zhang, G. Wang, J. Liu and L. Li, High-performance environmental adaptive microsupercapacitors from multifunctional hydrogel *via* modulating ionic hydration and hydrogen bonds, *Energy Storage Mater.*, 2023, **55**, 527–537.

27 C. Tang, M. Li, Y. Wang, Y. Zhang, Y. Yao, G. Wang, J. Liu and L. Li, Wide temperature range- and damage-tolerant microsupercapacitors from salt-tolerant, anti-freezing and self-healing organohydrogel *via* dynamic bonds modulation, *J. Energy Chem.*, 2023, **78**, 283–293.

28 Y. Pang, K. Zhang, X. Luan, B. Zhu, W. Shen, C. Xie, L. Li and J. Pang, Cellulose eutecticgel electrolytes based on ethylene glycol/zinc chloride deep eutectic solvent for flexible solid-state capacitors, *Chem. Eng. J.*, 2023, **477**, 146974.

29 C. Tian, J. Wang, R. Sun, T. Ali, H. Wang, B. B. Xie, Y. Zhong and Y. Hu, Improved Interfacial Ion Migration and Deposition through the Chain-Liquid Synergistic Effect by a Carboxylated Hydrogel Electrolyte for Stable Zinc Metal Anodes, *Angew. Chem., Int. Ed.*, 2023, **62**, e202310970.

30 J. Zheng, J. Liang, J. Xu, F. Lu, H. Yu, Y. Liu and R. Wang, Highly stretchable, anti-freezing, self-adhesion and self-healing zwitterionic hydrogel electrolytes for flexible electronic devices, *Chem. Eng. J.*, 2025, **508**, 161021.

31 J. Liu, F. Wang, W. Jiang, Q. Zhao, W. Li, C. Wang, S. Liu and Y. Liu, Polyzwitterionic hydrogel electrolytes *via* ultrafast autocatalytic gelation process for flexible Zn-Ion hybrid supercapacitors, *Chem. Eng. J.*, 2024, **483**, 149360.

32 Y. Sun, B. Liu, L. Liu, J. Lang and J. Qiu, A Low-Concentration and High Ionic Conductivity Aqueous Electrolyte toward Ultralow-Temperature Zinc-Ion Hybrid Capacitors, *Small Struct.*, 2023, **4**, 2200345.

33 X. Zhu, C. Ji, Q. Meng, H. Mi, Q. Yang, Z. Li, N. Yang and J. Qiu, Freeze-Tolerant Hydrogel Electrolyte with High Strength for Stable Operation of Flexible Zinc-Ion Hybrid Supercapacitors, *Small*, 2022, **18**, e2200055.

34 S. Huang, L. Hou, T. Li, Y. Jiao and P. Wu, Antifreezing Hydrogel Electrolyte with Ternary Hydrogen Bonding for High-Performance Zinc-Ion Batteries, *Adv. Mater.*, 2022, **34**, 2110140.

35 X. Yang, J. Zhou, B. Hao, B. Shen, Q. Qian, Z. Wang, C. Yan and T. Qian, Tailoring Cold-Resilient Electrolytes Driven by Mechanisms Underlying Ice Melting for Cryogenic Zn Batteries, *Adv. Mater.*, 2025, 2506537, DOI: **10.1002/adma.202506537**.

36 H. Su, Q. Guo, C. Qiao, X. Ji, L. Gai and L. Liu, Lignin-Alkali Metal Ion Self-Catalytic System Initiated Rapid Polymerization of Hydrogel Electrolyte with High Strength and Anti-Freezing Ability, *Adv. Funct. Mater.*, 2024, **34**, 2316274.

37 X. Zhao, Q. Guo, C. Gao, S. Nie and R. Sun, Bioinspired extreme environment adaptive hydrogel enabled by weakening hydrogen bonding, *Nano Energy*, 2025, **136**, 110748.

38 Y. T. Duan, J. D. Long, Y. H. Li, X. Tian, J. Q. Li, Z. Z. Fang, J. Wang and P. F. Huo, Lignin/soy protein isolate-based hydrogel polymer electrolytes for flexible solid-state supercapacitors with low temperature resistance, *J. Solid State Electrochem.*, 2024, **28**, 2021–2033.

39 Q. Hu, S. Cui, X. Shi, K. Sun, X. Wang, B. Liu, W. Sang, H. Peng and G. Ma, A self-healing, high stretchable and wide-temperature tolerance hydrogel electrolyte for high-performance supercapacitor, *Colloids Surf., A*, 2023, **663**, 131022.

40 J. Zeng, H. Chen, L. Dong, L. Wei and X. Guo, Designing of zwitterionic proline hydrogel electrolytes for anti-freezing supercapacitors, *J. Colloid Interface Sci.*, 2023, **652**, 856–865.

41 H. Peng, X. Gao, K. Sun, X. Xie, G. Ma, X. Zhou and Z. Lei, Physically cross-linked dual-network hydrogel electrolyte with high self-healing behavior and mechanical strength for wide-temperature tolerant flexible supercapacitor, *Chem. Eng. J.*, 2021, **422**, 130353.

42 J. H. Park, H. H. Rana, J. Y. Lee and H. S. Park, Renewable flexible supercapacitors based on all-lignin-based hydrogel electrolytes and nanofiber electrodes, *J. Mater. Chem. A*, 2019, **7**, 16962–16968.

43 S. Wu, D. Lou, H. Wang, D. Jiang, X. Fang, J. Meng, X. Sun and J. Li, One-pot synthesis of anti-freezing carrageenan/polyacrylamide double-network hydrogel electrolyte for low-temperature flexible supercapacitors, *Chem. Eng. J.*, 2022, **435**, 135057.

44 J. Nan, Y. Sun, F. Yang, Y. Zhang, Y. Li, Z. Wang, C. Wang, D. Wang, F. Chu, C. Wang, T. Zhu and J. Jiang, Coupling of Adhesion and Anti-Freezing Properties in Hydrogel Electrolytes for Low-Temperature Aqueous-Based Hybrid Capacitors, *Nano-Micro Lett.*, 2023, **16**, 22.

45 T. Gao, N. Li, Y. Yang, J. Li, P. Ji, Y. Zhou and J. Xu, Mechanical reliable, NIR light-induced rapid self-healing hydrogel electrolyte towards flexible zinc-ion hybrid supercapacitors with low-temperature adaptability and long service life, *J. Energy Chem.*, 2024, **92**, 63–73.